ISSN 1392-1207. MECHANIKA. Vol. 31, No. 4, 2025: 377–388

Vibration Characteristics Analysis of Rotor System with Permanent Magnet Drive Considering Misalignment and Unbalance

Honggang MU*, Huanle ZHAI*, Chungen SHEN, Luning WU*, Xiaomeng CHU*, Wuyan ZHU***

**Aviation Engineering Institute, Jiangsu Aviation Technical College, Zhenjiang, 212134, China, E-mail: muhonggang2010@163.com*

***School of Mechanical Engineering, Jiangsu University, Zhenjiang, 212013, China, E-mail: chungens@163.com*

https://doi.org/10.5755/j02.mech.40971

1. Introduction

In rotating machinery, the misalignment of the couplings or the unbalanced force caused by the mass eccentricity of a rotating part may lead to serious vibration of the rotor system, and even make the shaft to suddenly break. In order to reduce the vibration of the rotor system, it takes a lot of time to precisely align the couplings, especially for rigid couplings. Despite efforts to aligning interconnected shafts accurately, perfect alignment between shafts is challenging to maintain and achieve. With the emergence of permanent magnet coupling, this situation has been greatly changed. Permanent magnet coupling relies on the magnetic force of permanent magnet materials to achieve the transmission of speed and torque between the driver shaft and the driven shaft. Due to its excellent characteristics such as non-contact transmission, vibration isolation and noise reduction, low alignment accuracy and flexible starting, permanent magnet couplings have been widely used in rotating machinery systems in recent years. Compared with traditional mechanical couplings, such as elastic pin couplings, diaphragm couplings, etc., the permanent magnet couplings have lower requirements for the alignment accuracy of the driver shaft and the driven shaft. However, when there is a large axial or radial misalignment, it will inevitably have a certain impact on the vibration characteristics of the rotor system. Especially for high speed and light load conditions, misalignment is the main factor leading to the failure of the coupling and its system. Many research results show that the misalignment faults account for more than 60% of the total failures of rotating machinery systems. In addition, the unbalanced force caused by the mass eccentricity of the rotating part will also lead to vibration of the rotor system. Therefore, it is of great significance for engineering application to study the effects of misalignment and unbalance on vibration characteristics of rotor system.

Many researchers have carried out a lot of studies on the vibration characteristics of rotor system. Ma et al. [1] developed the finite element model (FEM) of rotor system with coupling parallel misalignment based on Timoshenko beam theory, and found that the existence of parallel misalignment can intensify the slight collision. Wang et al. [2] investigated the influences of initial clearance, mass eccentricity and inter-shaft bearing stiffness on the dynamic characteristics of dual-rotor bearing system. Sawalhi et al. [3] presented a parallel misalignment model and coupling bending stiffness measurement of a rotor-bearing system. Liu et al. [4] studied the dynamic effects of structure parameters and the external load on the stiffness and contact state of the aero-engine rotor joints with nonlinear finite-element method. Lu et al. [5] developed a nonlinear dynamic and lumped parameter model of the rotor bearing system, and analyzed the effects of rotor hybrid eccentricity and bearing clearance on dynamic characteristics of the rotor bearing system of a permanent magnet motorized spindle. Xue et al. [6] investigated the non-linear dynamic meshing force of spline coupling in aero-engine under different misalignment and mass eccentricity. Wang et al. [7] used Newmark-β method to solve the nonlinear equations of rotor system, and studied the dynamic analysis of rotor system with misalignment and unbalance coupled faults. Mohamed et al. [8] discussed the simultaneous effect of imbalance and misalignment on the vibration spectra of rotating machinery, and developed a numerical model in order to obtain the time and frequency responses of the rotor-coupling-bearing system. Li et al. [9] derived the motion equations of the rotor system based on Lagrange method after taking into account a holonomic constraint characterized by the parallel misalignment between two rotors, and discussed the dynamic responses of the rotor system. Wang et al. [10] derived a unified expression for the unbalanced magnetic pull of the motor under various pole pairs and air-gap eccentricities, and analyzed the effect of the unbalanced magnetic pull and harmonic response characteristics on the rotor. Huang et al. [11] established a dynamic model for the rotor system coupled with parallel misalignment and mass eccentricity, and investigated the dynamic behaviors of rotor system using numerical integral method. Deepak et al. [12] presented the results of Harmonic analysis of the Aluminium shaft rotor bearing system with rigid coupling under parallel misalignment using FEA. Wang et al. [13] developed the dual-rotor dynamic model with unbalance-misalignment and investigated the effects of different rotational angular speeds, mass eccentricity, misalignment angle and parallel misalignment on dynamic characteristics. Wang et al. [14] proposed a five-degree of freedom (5-DOF) nonlinear force model considering bearing misalignment. The model comprehensively considered the parallel and angular misalignment, static and dynamic misalignment, inner ring and outer ring misalignment. Xie et al. [15] clarified the rotor-dynamic and vibration performances of a new bearings-rotor coupled system, and analyzed the influences of rotating speed, external load, length-diameter ratio and other parameters on the lubrication performances and supporting behaviors of the bearings. Chen et al. [16] explored the unbalanced magnetic pull equation of the permanent magnet synchronous motor rotor,

and studied the effects of electromagnetic stiffness coefficient, mass unbalance parameters and damping on the overall dynamic response.

As can be seen from the above published literatures, there are many studies on the vibration characteristics of rotor systems. However, there are few researches on the vibration characteristics of rotor system with permanent magnet drive. In view of the wide applications of permanent magnet coupling in mechanical transmission systems, it is necessary to study the vibration characteristics of rotor system with permanent magnet drive. In this paper, the vibration characteristics of centrifugal pump rotor system driven by asynchronous disc permanent magnet coupling (ADPMC) is studied. This paper aims to analyze the effect of misalignment and unbalance on the vibration characteristics of centrifugal pump rotor system, and provide references for the practical engineering application of ADPMC.

2. Model of the Centrifugal Pump Rotor System

The three-dimensional model of the centrifugal pump rotor system driven by ADPMC is shown in Fig. 1. The motor power used to drive the rotor system is rated at 55 kW, and the rated operating speed is 3000 r/min. As can be seen from Fig. 1, the centrifugal pump rotor system mainly includes the driver rotor of ADPMC, driven rotor of ADPMC, angular contact ball bearing I, angular contact ball bearing II, centrifugal pump shaft, cylindrical roller bearing III and impeller. A pair of angular contact ball bearing I and bearing II are installed back-to-back on the left journal of the centrifugal pump shaft. A set of cylindrical roller bearing III is installed on the right journal of the centrifugal pump shaft. The ADPMC is characterized by an asynchronous disk structure. Its driver rotor is a conductor disk structure, and its driven rotor is a permanent magnet disk structure. The axial air gap is arranged between the conductor disk and the permanent magnet disk, and the air gap is full of the magnetic field line. The driver rotor and driven rotor of ADPMC are respectively connected with the motor shaft and the centrifugal pump shaft through the flange sleeves. The driver rotor and driven rotor of ADPMC are transmitted asynchronously during operating.

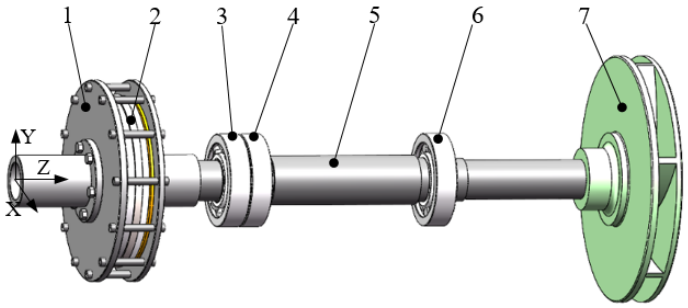

Fig. 1 Three-dimensional model of centrifugal pump rotor system: *1* – driver rotor of ADPMC, *2* – driven rotor of ADPMC, *3* – bearing I, *4* – bearing II, *5* – centrifugal pump shaft, *6* – bearing III, *7* – impeller

3. Calculation of Unbalanced Magnetic Pull of ADPMC

3.1. Structure and parameters of ADPMC

When a pair of permanent magnetic disk and conductor disk of permanent magnet coupling are coupled, a large axial force will be generated. In order to reduce the adverse effect of axial force on bearings in rotor system, ADPMC usually adopts standard dual-coupled structure in engineering application. Fig. 2 shows parametric model of the dual-coupled disk of ADPMC in rotor system.

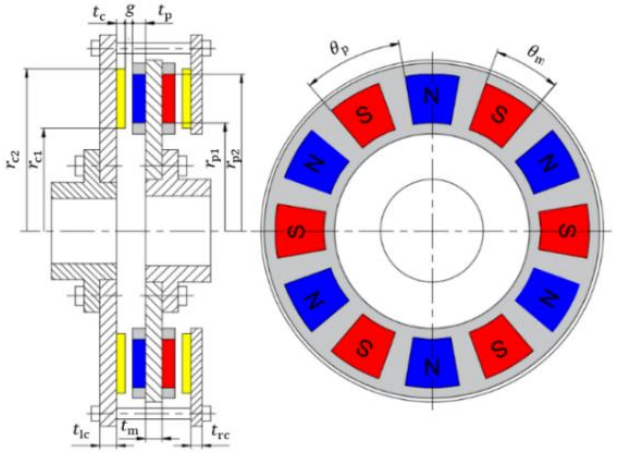

Fig. 2 Parametric model of ADPMC

The driver rotor of ADPMC is a double conductor disk. The left conductor disk and the right conductor disk are fixed to the left yoke iron and the right yoke iron, respectively. Then, the left conductor disk and right conductor disk are rigidly connected. The driven rotor of ADPMC is a double permanent magnet disk. The left and right permanent magnets are embedded in the left and right aluminium alloy positioning disks respectively, and then they are fixed to the middle yoke iron as a whole. The left and right permanent magnets are all axially magnetized, and the magnetic circuit is an alternating arrangement of N-S magnetic poles. The technical parameters of ADPMC are listed in Table 1.

3.2. Calculation of axial magnetic pull of ADPMC

In order to study the effect of misalignment on the vibration characteristics of centrifugal pump rotor system, it is necessary to calculate the unbalanced magnetic pull caused by the misalignment of ADPMC. When the ADPMC is installed, the axial, radial, or angular misalignment may occur because the position of the driver shaft and the driven shaft is not accurate. In this paper, the effects of axial and radial misalignment of ADPMC on the vibration characteristics of rotor system are discussed. Firstly, the effect of axial misalignment of ADPMC on vibration characteristics of centrifugal pump rotor system is studied. When the ADPMC has axial misalignment, it will lead to an axial unbalanced

Table 1

Technical parameters of ADPMC

Parameter name	Value	Parameter name	Value
Inner radius of permanent magnet r_{p1}, mm	80	Inner radius of conductor disk r_{c1}, mm	74
Outer radius of permanent magnet r_{p2}, mm	130	Outer radius of conductor disk r_{c2}, mm	136
Thickness of permanent magnet t_p, mm	12	Thickness of conductor disk t_c, mm	5
Thickness of middle yoke iron t_m, mm	12	Thickness of left yoke iron t_{lc}, mm	12
Magnetic poles of left disk p	12	Thickness of right yoke iron t_{rc}, mm	10
Magnetic poles of right disk p	12	Pole pitch angle θ_p, °	30
Air gap thickness g, mm	3.5	Pole arc angle θ_m, °	20
Remanence of permanent magnet B_r, mT	1300	Relative permeability of permanent magnet μ_{rp}	1.1123
Coercivity of permanent magnet H_{cb}, kA/m	930	Relative permeability of copper conductor μ_{rc}	0.999991
Conductivity of copper conductor σ_c, S/m	5.8×10^7	Relative permeability of aluminium alloy μ_{ra}	1.000021
Vacuum permeability μ_0, H/m	$4\pi\times10^{-7}$	Operating temperature T, °C	20

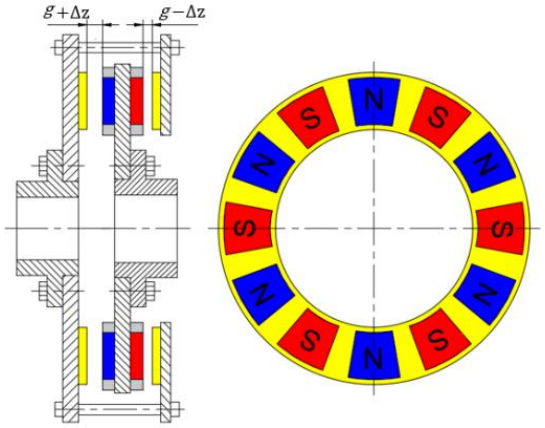

Fig. 3 Diagram of ADPMC with axial misalignment

magnetic pull. Fig. 3 shows the axial misalignment Δz between the permanent magnet disk and the conductor disk of ADPMC.

Compared to the ideal air gap thickness g, the left air gap thickness increases by Δz and naturally the right air gap thickness decreases by Δz. According to the technical parameters of ADPMC in Table 1, the three-dimensional FEM of ADPMC is established. The three-dimensional transient magnetic field of ADPMC is simulated by finite element software. The magnetic flux density distribution of conductor disk and the axial unbalanced magnetic pull are obtained when there are different axial misalignments.

Fig. 4 shows the magnetic flux density distribution of the left and right conductor disks of ADPMC when the axial misalignment Δz is 1 mm, 2 mm and 3 mm. It can be seen from Fig. 4 that when the axial misalignment Δz is 1 mm, the maximum magnetic flux density of the left and right conductor disks of the ADPMC are 806 mT and 1033 mT, respectively. When the axial misalignment Δz is 2 mm, the maximum magnetic flux density of the left and right conductor disks of the ADPMC is 761 mT and 1101 mT, respectively. Accordingly, when the axial misalignment Δz is 3 mm, the maximum magnetic flux density of the left and right conductor disks of the ADPMC is 714 mT and 1183 mT, respectively. Therefore, with the increase of axial misalignment Δz, the maximum magnetic flux density of the left conductor disk gradually decreases, while the maximum magnetic flux density of the right

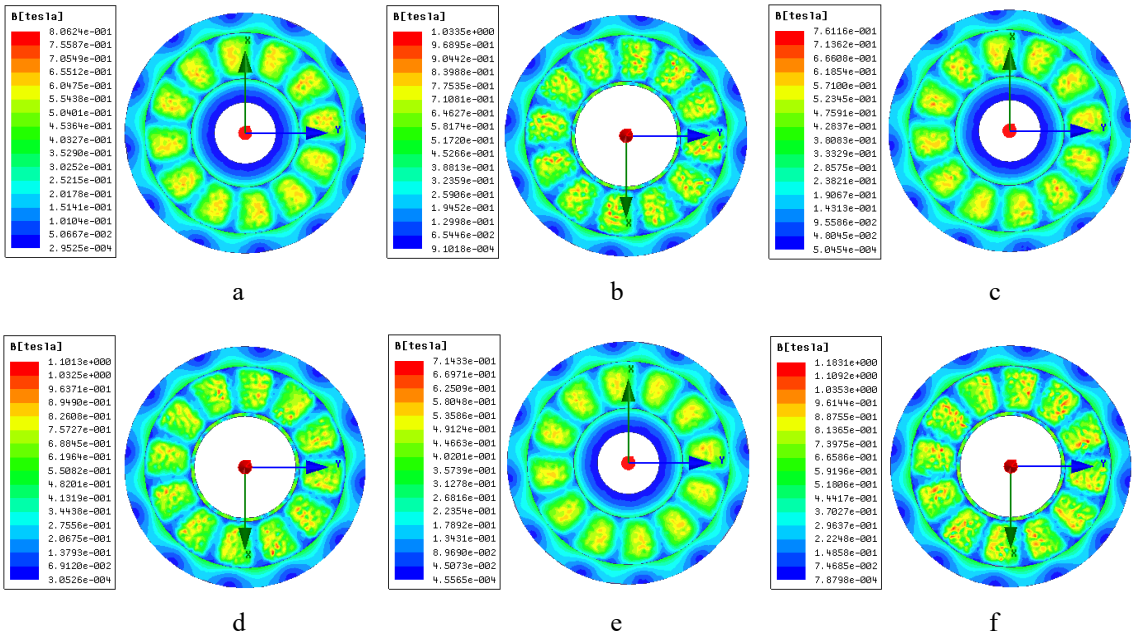

Fig. 4 Magnetic flux density distribution of conductor disk of ADPMC with different axial misalignments: a – left disk (Δz = 1 mm), b – right disk (Δz = 1 mm), c – left disk (Δz = 2 mm), d – right disk (Δz = 2 mm), e – left disk (Δz = 3 mm), f – right disk (Δz = 3 mm)

conductor disk gradually increases, which is related to the change of the air gap thickness between the conductor disk and the permanent magnet disk.

Fig. 5 shows the axial unbalanced magnetic pull of ADPMC with different axial misalignments. As can be seen from Fig. 5, with the increase of axial misalignment of ADPMC, the axial unbalanced magnetic pull between the conductor disk and the permanent magnetic disk presents a nonlinear and sharply rising trend. When the axial misalignment Δz is 1 mm, 2 mm and 3 mm, the axial unbalanced magnetic pull F_A between the driver rotor and the driven rotor of ADPMC is 780 N, 1220 N and 2588 N, respectively. It can be seen that ADPMC is sensitive to axial misalignment Δz.

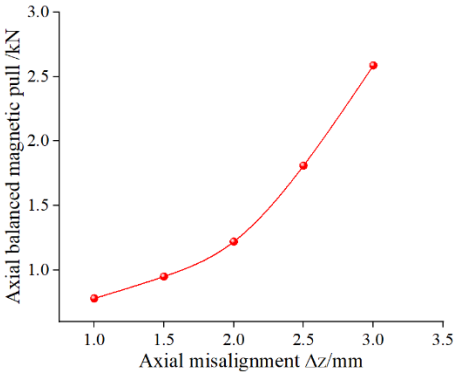

Fig. 5 Axial unbalanced magnetic pull of ADPMC

With the slight increase of axial misalignment, the axial unbalanced magnetic pull F_A increases significantly. The axial unbalanced magnetic pull eventually acts on the bearings, which will lead to the internal friction of the bearings to intensify, and even the inner and outer ring deformation, thus affecting the life of the bearings. Consequently, a large axial misalignment of ADPMC is not allowed in engineering applications.

3.3. Calculation of radial magnetic pull of ADPMC

In order to study the effect of radial misalignment of ADPMC on the vibration characteristic of rotor system, it is necessary to calculate the radial unbalanced magnetic pull between the driver rotor and driven rotor of ADPMC under different radial misalignments. Fig. 6 shows the structure diagram of ADPMC with radial misalignment.

Similarly, according to the technical parameters of ADPMC in Table 1, its three-dimensional FEM is established. The three-dimensional transient magnetic field of ADPMC is simulated by finite element software, and radial unbalanced magnetic pull and the magnetic flux density of conductor disk are solved when there are different radial misalignments. Fig. 7 shows the magnetic flux density distribution of the left and right conductor disks of ADPMC when the radial misalignment Δy is 1 mm, 3 mm and 5 mm. As can be seen from Fig. 7, when the radial misalignment Δy is 1 mm, the maximum magnetic flux density of the left and right conductor disks of the ADPMC are 851 mT and 936 mT, respectively. When the radial misalignment Δy is 3 mm, the maximum magnetic flux density of the left and

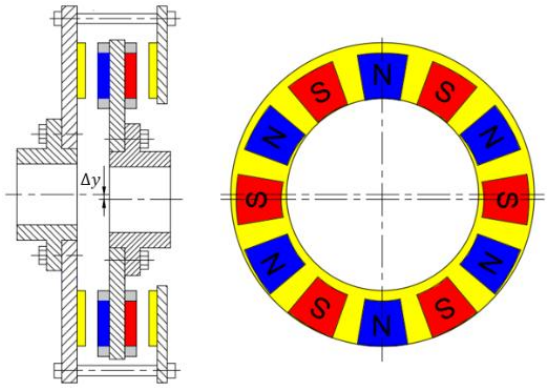

Fig. 6 Diagram of ADPMC with radial misalignment

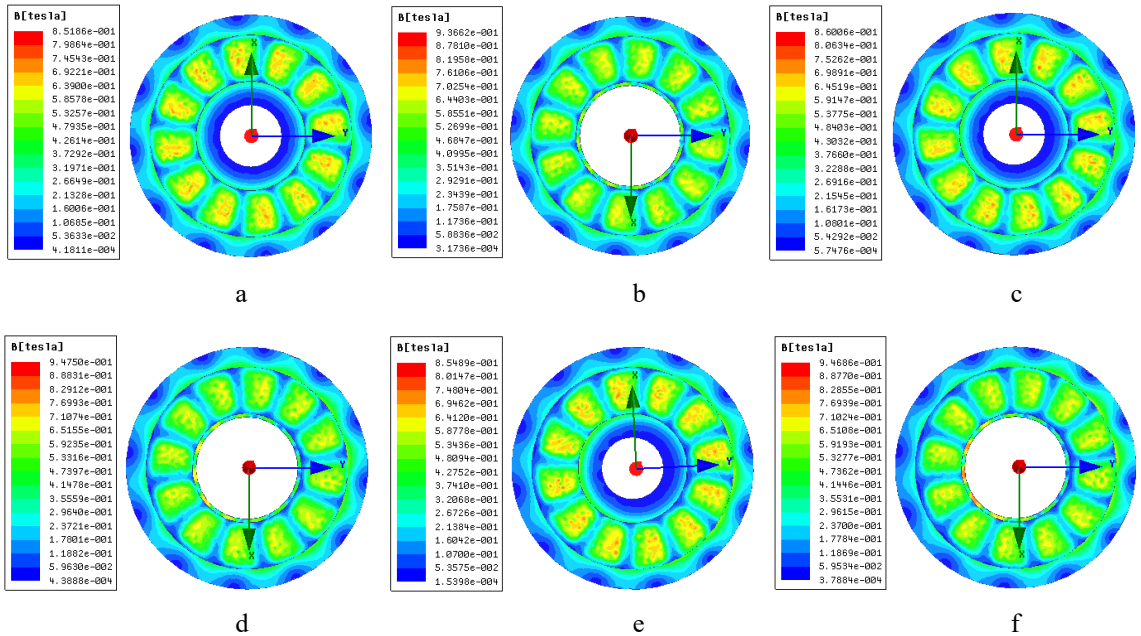

Fig. 7 Magnetic flux density of conductor disk of ADPMC with different radial misalignments: a – left disk (Δy = 1 mm), b – right disk (Δy = 1 mm), c – left disk (Δy = 3 mm), d – right disk (Δy = 3 mm), e – left disk (Δy = 5 mm), f – right disk (Δy= 5 mm)

right conductor disks of the ADPMC are 860 mT and 947 mT, respectively. Accordingly, when the radial misalignment Δy is 5 mm, the maximum magnetic flux density of the left and right conductor disks of the ADPMC are 854 mT and 946 mT, respectively. Therefore, it can be seen that with the change of radial misalignment Δy, there is no significant effect on the maximum magnetic flux density of the left and right conductor disks. Obviously, this is related to the constant air gap thickness between the permanent magnet disk and the conductor disk.

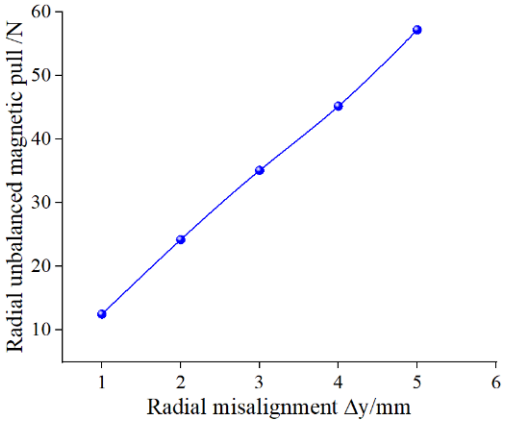

Fig. 8 Radial unbalanced magnetic pull of ADPMC

Fig. 8 shows the radial unbalanced magnetic pull between the driver rotor and the driven rotor of ADPMC when there are different radial misalignments. As can be seen from Fig. 8, with the increase of radial misalignment Δy, the radial unbalanced magnetic pull between the conductor disk and the permanent magnetic disk shows a slow linear increasing trend.

When the radial misalignment Δy is 1 mm, 3 mm and 5 mm, the radial unbalanced magnetic pull of ADPMC are 12.5 N, 35.2 N and 57.3 N, respectively. Obviously, it can be seen that the radial unbalanced magnetic pull caused by the radial misalignment is relatively small, which is related to the use of axial magnetic coupling between the driver rotor and the driven rotor of ADPMC. Therefore, a large radial misalignment of ADPMC can be allowed in engineering applications.

4. Calculation of Radial Support Stiffness of Bearing

4.1. Axial force of angular contact ball bearing

The radial support stiffness of angular contact ball bearing is related to the axial force, so the axial force of bearing is calculated first. According to the structure and force situation of the centrifugal pump rotor system, the force diagram of the rotor system is drawn as shown in Fig. 9. When the dynamic analysis of centrifugal pump rotor system is carried out, the driver rotor and the driven rotor of ADPMC can be isolated. It means that only the driven rotor of ADPMC is included in the rotor system for vibration characteristics analysis.

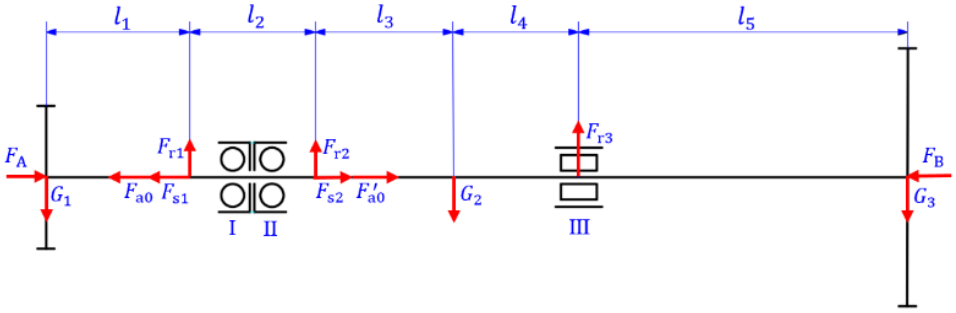

Fig. 9 Force diagram of centrifugal pump rotor system

As shown in Fig. 9, a pair of angular contact ball bearing I and bearing II are arranged back-to-back on the left journal of the centrifugal pump shaft. If the axial preload force F_{a0} is applied to angular contact ball bearing, the axial preload force of bearing I and bearing II are equal in magnitude and opposite in direction, where F_{a0} is 150 N. The weight G_1 of the driven rotor of ADPMC is 170 N, and the axial unbalanced magnetic pull it bears is F_A. The weight G_2 of the centrifugal pump shaft is 290 N. The weight G_3 of the impeller is 250 N, and the operating axial force F_B generated by the impeller is 600 N. The radial support reaction forces on bearing I, bearing II and bearing III are set as F_{r1}, F_{r2} and F_{r3} respectively, and the axial derived forces generated by bearing I and bearing II are F_{s1} and F_{s2}. The distance parameters between the operating points of each radial force are as follows, l_1 = 149 mm, l_2 = 126 mm, l_3 = 139 mm, l_4 = 126 mm, l_5 = 330 mm. According to the equilibrium conditions of force and moment, the equations are listed as follows:

$$\begin{cases} \sum F_{ri} = 0 \\ \sum M_i = 0 \end{cases}. \tag{1}$$

The results of radial support reaction forces of bearing I, bearing II and bearing III are calculated respectively, where F_{r1} = 70 N, F_{r2} = 70 N, F_{r3} = 570 N.

When the contact angle of angular contact ball bearing I and bearing II are both 40 degrees, the axial derived forces of bearing I and bearing II can be calculated according to the following equation.

$$F_{si} = 1.14 F_{ri}. \tag{2}$$

According to the above formula, the axial derived force of bearing I is calculated, where F_{s1} = 79.8 N. At the same time, the axial derived force of bearing II is calculated, where F_{s2} = 79.8 N.

Then, the axial force of angular contact ball bearing I and bearing II are calculated respectively when the axial misalignment Δz is 1 mm, 2 mm and 3 mm. As a contrast, the axial force of the angular contact ball bearing without axial misalignment is also calculated, where $\Delta z = 0$. The resultant force of the axial unbalanced magnetic pull, axial derived force, axial preload force and operating axial force is calculated to determine that the angular contact ball bearing I and bearing II are in a relatively pressed or relaxed state, and the axial force of bearing I and bearing II are further calculated. For the above four operating conditions, the axial forces of angular contact ball bearing I and bearing II are calculated as shown in Table 2.

Table 2

Axial force of angular contact ball bearing

Axial misalignment Δz, mm	Axial force of bearing I F_{a1}, N	Axial force of bearing II F_{a2}, N
0	229.8	829.8
1	409.8	229.8
2	849.8	229.8
3	2217.8	229.8

4.2. Radial support stiffness of bearings

In order to analyze the vibration characteristics of centrifugal pump rotor system, it is necessary to calculate the radial support stiffness of each bearing.

Bearing I, bearing II and bearing III in the centrifugal pump rotor system are all treated as elastic supports in this paper. The structure diagram of the elastic support of bearing to shaft is shown in Fig. 10. As shown in Fig. 10, c represents the damping coefficient and K represents the stiffness of the elastic support.

According to the reference [17], the radial support stiffness K_{r1} of the angular contact ball bearing I is calculated as follows. In order to simplify the calculation,

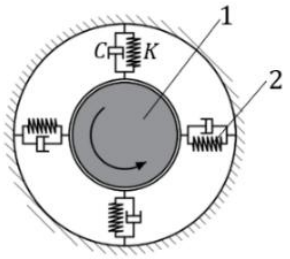

Fig. 10 Elastic support diagram of the bearing to the shaft: *1* – shaft, *2* – elastic support

the influence of damping is not considered, so the damping coefficient c is set to zero.

$$K_{r1} = 17.7236\xi \cdot \sqrt[3]{Z^2 \times D_w} \cdot \frac{\cos^2 \alpha_0}{\sqrt[3]{\sin \alpha_0}} \cdot \sqrt[3]{F_{a1}}, \tag{3}$$

where ξ represents the correction coefficient. Z represents the number of angular contact ball bearing rolling element. D_w represents the diameter of angular contact ball bearing rolling element, α_0 represents the operating contact angle of angular contact ball bearing, F_{a1} represents the axial force of the angular contact ball bearing.

Cylindrical roller bearing III is also treated as elastic support. The radial support stiffness K_{r3} of cylindrical roller bearing III can be regarded as the result of the oil film stiffness K_f and the contact stiffness K_n in series, and its calculation formula expressed in reference [18] is as follows

$$K_{r3} = \frac{1}{\frac{1}{K_f} + \frac{1}{K_n}} = \frac{1}{0.13CF_{r3}^{-1.13} + B\ln F_{r3} + A + B}. \tag{4}$$

In the above formula, the undetermined parameters A, B and C are calculated respectively by the following formula:

$$A = \frac{8.16}{E'Zl}\left[\frac{1}{\pi}\ln 0.39E'Zl\left(R_1 + r\right) + 1.15 - 0.5\ln\frac{8.16rR_2}{E'\left(R_2 - r\right)Zl}\right], \tag{5}$$

$$B = -6.68\frac{1}{E'Zl}, \tag{6}$$

$$C = 0.28\alpha^{0.54}\left(\mu_0 n_i\right)^{0.7} r^{0.43}\left(R_1 + r\right)^{0.7}\left[\left(1-\gamma\right)^{1.13}\left(1+\gamma\right)^{0.7} + \left(1+\gamma\right)^{1.13}\left(1-\gamma\right)^{0.7}\right]E'^{-0.03}Z^{0.13}l^{0.13}. \tag{7}$$

Here R_1 and R_2 represents the inner and outer raceway radius of cylindrical roller bearing, r represents the radius of the cylindrical roller element, E' represents the comprehensive modulus of elasticity of material, define $E' = E / (1-\nu^2)$, E represents the modulus of elasticity of material, ν represents Poisson's ratio, F_{r3} represents the radial force on the cylindrical roller bearing, l represents the effective contact length of the cylindrical roller, Z represents the number of cylindrical rollers, n_i represents the speed of the inner raceway, μ_0 represents the viscosity of lubricating oil, α represents the viscosity coefficient. In addition, define $\gamma = r / (R_1 + r)$.

Considering that the angular contact ball bearing cannot be subjected to large axial force in the engineering practice, otherwise it will greatly affect its life. Therefore, the axial misalignment of ADPMC should not be too large. Instead, it is advisable to take a smaller value. When the axial misalignment Δz of ADPMC is 1 mm and 2 mm, the

Table 3

Radial support stiffness of the bearings

Axial misalignment of ADPMC Δz, mm	Radial support stiffness of bearing I K_{r1}, N/μm	Radial support stiffness of bearing II K_{r2}, N/μm	Radial support stiffness of bearing III K_{r3}, N/μm
0	193.3	296.5	645
1	234.4	193.3	645
2	298.9	193.3	645

radial support stiffness of bearing I, bearing II and bearing III are calculated respectively. As a comparison, the axial support stiffness of each bearing is also calculated when ADPMC has no axial misalignment, that is, $\Delta z = 0$. In the above three operating conditions, the radial support stiffness of each bearing is listed in Table 3.

5. Modal Analysis of Centrifugal Pump Rotor System

In the following text, a modal analysis of centrifugal pump rotor system will be conducted. The purpose of modal analysis is to solve the natural frequencies and modal shapes of the rotor system. The three-dimensional FEM of the rotor system including the driven rotor of ADPMC, centrifugal pump shaft and impeller is established. The bearings at the left and right journal of the centrifugal pump shaft are taken as the elastic supports. The radial support stiffness of each bearing is shown in Table 3. The modal analysis of centrifugal pump rotor system is solved by ANSYS simulation software to obtain the natural frequencies and modal shapes of rotor system when the axial misalignment Δz is 0 mm, 1 mm and 2 mm.The first six order natural frequencies of the centrifugal pump rotor system under the above three operating conditions are listed in Table 4.

As can be seen from Table 4, when the axial misalignment Δz of ADPMC is 0 mm, 1 mm and 2 mm respectively, the natural frequencies of the centrifugal pump rotor system with the same modal order are basically the same, which is related to the arrangement of bearings. Since a pair of angular contact ball bearing I and bearing II are centrally arranged back-to-back on the left journal of the centrifugal pump shaft, the radial support stiffness of the bearing combination will not be affected whether the bearing I is relatively compressed and the bearing II is relaxed, or vice versa. A cylindrical roller bearing is arranged at the right journal of the centrifugal pump shaft, and its radial support stiffness has nothing to do with the axial force. In addition, it can be seen from Table 4 that the natural frequencies of the 3rd and 4th order of the rotor system are the same, and that of the 5th and 6th order of the rotor system are the same, which represents the vibration of the rotor system in the orthogonal direction.

Table 4

Natural frequency of centrifugal pump rotor system

Modal order	Natural frequencies f/Hz		
	Δz = 0 mm	Δz = 1 mm	Δz = 2 mm
1st order	1.087	1.035	1.035
2nd order	22.22	20.95	20.95
3rd order	78.43	78.19	78.36
4th order	78.43	78.19	78.37
5th order	193.52	194.04	199.77
6th order	193.53	194.05	199.77

The first six modal shapes of the centrifugal pump rotor system are shown in Fig. 11. Among them, Fig. 11, a shows the 1st order modal shape of rotor system, which mainly represents the angular torsional vibration of the permanent magnet disk and the impeller. Fig. 11, b shows the 2nd order modal shape of rotor system, which mainly represents the axial vibration of the rotor system. Fig. 11, c and Fig. 11, d shows the 3rd order and 4th order modal shapes of rotor system respectively, which are also the 1st order bending modal shapes of the rotor system. They mainly represent the vibration of the impeller in the orthogonal

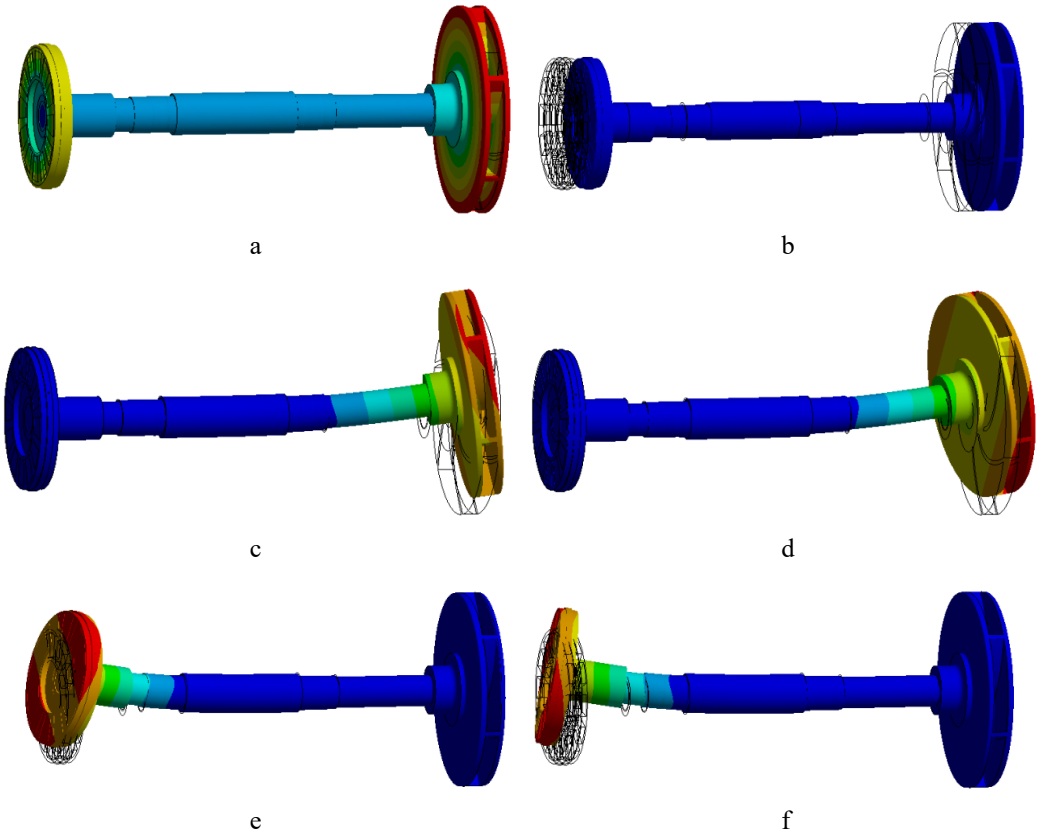

Fig. 11 Modal shapes of centrifugal pump rotor system: a – 1st order, b – 2nd order, c – 3rd order, d – 4th order, e – 5th order, f – 6th order

direction. Similarly, Fig. 11, e and Fig. 11, f shows the 5th order and 6th order modal shapes of rotor system, which are also the 2nd order bending modal shapes of the rotor system. They mainly represent the vibration of the permanent magnet disk in the orthogonal direction. According to the 1st order and 2nd order bending modal shapes of rotor system in Fig. 11, c and Fig. 11, e, the bending vibration of the impeller and the permanent magnet disk can be reduced by increasing the radial support stiffness of the centrifugal pump shaft.

6. Harmonic Response Analysis of Centrifugal Pump Rotor System

In order to analyze the harmonic response characteristics of the centrifugal pump rotor system, it is necessary to define the excitation sources. The main excitation sources that cause vibration of rotor system include the unbalanced magnetic pull, the unbalanced force and the exciting force. Among them, the unbalanced magnetic pull is caused by ADPMC misalignment, the unbalanced force is caused by mass eccentricity of the impeller at high speed [19], and the exciting force is caused by some other factors such as wear and aging of bearing and so on. In this paper, the effects of the first two excitation sources on the radial vibration characteristics of the rotor system will be studied, and the radial vibration response of the rotor system caused by a single excitation source and dual excitation sources will be considered respectively.

According to the above analysis, the axial misalignment of ADPMC will give rise to large axial unbalanced magnetic pull, which will affect the radial support stiffness of angular contact ball bearings. The radial misalignment of ADPMC will bring about a certain radial unbalanced magnetic pull, which will cause radial vibration of the centrifugal pump rotor system. When ADPMC is installed, there may be both axial misalignment and radial misalignment. But the unbalanced magnetic pull is more sensitive to the axial misalignment of ADPMC. Therefore, the axial misalignment of ADPMC should be as small as possible in engineering applications. In the following, the effects of different excitation sources on the radial vibration characteristics of rotor system are discussed only when the axial misalignment Δz of ADPMC is 1 mm.

Fig. 12 shows the three-dimensional model of the centrifugal pump rotor system for harmonic response analysis. In the same way, bearing I, bearing II and bearing III are all considered as elastic supports in harmonic response analysis. The radial unbalanced magnetic pull F_M is applied to the rim of the permanent magnet disk as an exciting source, and the unbalanced force F_C caused by the mass eccentricity of the impeller is applied to the rim of the impeller as another exciting source. Monitoring point M_1 is arranged on the left journal of centrifugal pump shaft and monitoring point M_2 is arranged on the right journal of centrifugal pump shaft. The vibration characteristics of rotor system can be represented by the radial vibration displacements of these two points.

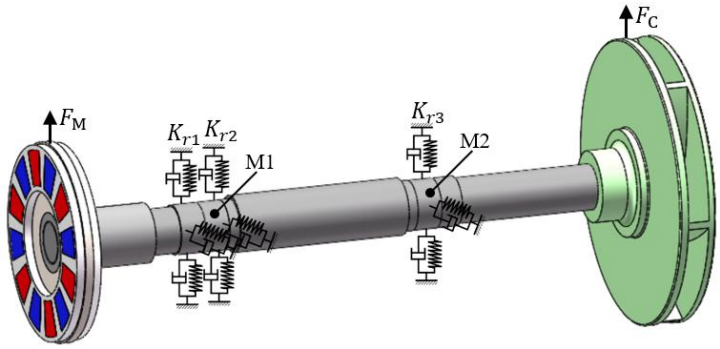

Fig. 12 Harmonic response analysis model of centrifugal pump rotor system

The vibration response analysis of the centrifugal pump rotor system is carried out under two kinds of operating conditions. The condition 1 – the effect of a single excitation source on the vibration characteristics of the rotor system is analyzed. That is, only the radial unbalanced magnetic pull F_M caused by the misalignment of ADPMC is applied to the rotor system for harmonic response analysis. In this case, the unbalanced force F_C is set to zero. The condition 2 – the effects of the combination of dual excitation sources on the vibration characteristics of the rotor system is studied. That is, the radial unbalanced magnetic pull F_M and the unbalanced force F_C are applied to the rotor system together. The vibration displacements of points M_1 and M_2 are extracted to represent vibration characteristics of the rotor system at the same time.

Firstly, the effect of single excitation source on vibration characteristics of rotor system is studied. When the radial misalignment Δy of ADPMC is 1 mm, 2 mm, 3 mm, 4 mm and 5 mm, the radial unbalanced magnetic pull F_M caused by misalignment is applied to the rotor system respectively to analyze the harmonic response characteristics.

Fig. 13 shows the vibration spectrum of points M_1 and M_2 obtained by harmonic response analysis. As can be seen from Fig. 13, when the frequency of excitation source is 78 Hz, that is, near the 1st order bending critical speed of the rotor system, the vibration displacements of M_1 and M_2 are small. However, when the frequency of excitation source is approximately 194 Hz, that is, near the 2nd order bending critical speed of the rotor system, the vibration displacements of M_1 and M_2 are large. Moreover, with the increase of the radial misalignment of ADPMC, the vibration displacements of points M_1 and M_2 show an increasing trend, especially near the 2nd order bending critical speed. It can be seen that near the 2nd order bending critical speed, when the radial misalignment Δy of ADPMC is 1 mm, 3 mm and 5 mm, the vibration displacement of M_1 is 9.3 μm, 26.3 μm and 42.9 μm, and the vibration displacement of M_2 is 2.28 μm, 6.42 μm and 10.4 μm respectively.

The ADPMC works in an asynchronous drive mode, and the slip rate between the driver end and the driven end is about 5%. The rated operating speed of the drive motor is 3000 r/min. Accordingly, the operating speed of the rotor system is 2850 r/min, and the corresponding operating frequency is 47.5 Hz. As can be seen from Fig. 13, when the radial misalignment Δy of ADPMC is 1 mm, 2 mm, 3 mm, 4 mm or 5 mm, the vibration displacements of points M_1 and M_2 are relatively small near the operating frequency of 47.5 Hz. Obviously, the radial misalignment of ADPMC has no significant effect on the vibration of rotor system, and even allows the existence of millimeter level radial misalignment of ADPMC, which fully indicates that ADPMC has a good vibration isolation characteristic between the driver shaft and the driven shaft in rotating machinery. Therefore, ADPMC has been widely applied in mechanical transmission systems, especially in those with strict requirements for vibration.

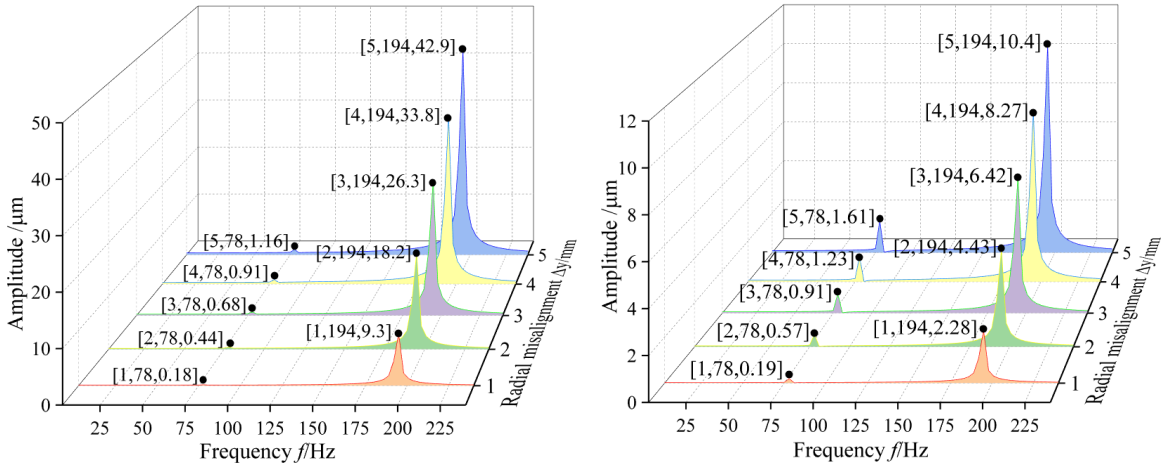

a b

Fig. 13 Vibration spectrum diagrams of monitoring points under single excitation source: a – vibration spectrum of point M_1, b – vibration spectrum of M_2

Secondly, the effect of dual excitation sources on the vibration characteristics of the centrifugal pump rotor system is analyzed. In other words, the radial unbalanced magnetic force F_M and the unbalanced force F_C caused by the mass eccentricity of the impeller are jointly applied to the rotor system for harmonic response analysis. To simplify the calculation, in this paper, when the radial misalignment of ADPMC is 1 mm, 3 mm and 5 mm, the resulting unbalanced magnetic pull F_M is applied to the rim of the permanent magnet disk, respectively. Meanwhile, the unbalanced force F_C caused by the mass eccentricity of the impeller is applied to the rim of impeller, and the unbalanced force F_C is 10 N, 20 N, 30 N, 40 N and 50 N respectively.

Fig. 14 shows the vibration spectrums of points M_1 and M_2 under the action of dual excitation sources. Fig. 14, a shows the vibration spectrum of point M_1 when the radial misalignment of ADPMC is 1 mm. As can be seen from Fig. 14, a, when the unbalanced magnetic pull F_M is constant, with the increase of the unbalanced force F_C, the vibration response of point M_1 at the 3rd order natural frequency increases significantly, but the vibration response of point M_1 at the 5th order natural frequency is almost unchanged. When the unbalanced force F_C is 50 N, the vibration response of point M_1 at the 3rd order natural frequency is 43.4 μm, and the vibration response of point M_1 at the 5th order natural frequency is 9.32 μm.

Fig. 14, b shows the vibration spectrum of point M_2 when the radial misalignment of ADPMC is 1 mm. It can be seen that the vibration response characteristics of points M_1 and M_2 are similar. However, the vibration response of point M_2 at the 5th order natural frequency is smaller. When the unbalanced force F_C is 50 N, the vibration response of point M_2 is 98.1 μm at the 3rd order natural frequency and the vibration response of point M_2 is 2.20 μm at the 5th order natural frequency.

Fig. 14, c shows the vibration spectrum diagram of point M_1 when the radial misalignment Δy of ADPMC is 3 mm. Fig. 14, e shows the vibration spectrum diagram of point M_1 when the radial misalignment Δy of ADPMC is 5 mm. Combined with Fig. 14, a, it can be seen that with the radial misalignment of ADPMC increases, the vibration response of point M_1 at the 3rd order natural frequency is basically unchanged, while the vibration response of point M_1 at the 5th order natural frequency increases significantly. When the radial misalignment Δy of ADPMC is 5 mm and the unbalanced force F_C is 50 N, the vibration response of point M_1 is 42.4 μm at the 3rd order natural frequency and the vibration response of point M_1 is 42.8 μm at the 5th order natural frequency.

Fig. 14, d shows the vibration spectrum diagram of point M_2 when the radial misalignment Δy of ADPMC is 3 mm. Fig. 14, f shows the vibration spectrum diagram of point M_2 when the radial misalignment Δy of ADPMC is 5 mm. Meanwhile, combined with Fig. 14, b, it can be seen that with the radial misalignment of ADPMC increases, the vibration response of point M_2 at the 3rd order natural frequency is basically unchanged, while the vibration response of point M_2 at the 5th order natural frequency increases slightly. When the radial misalignment Δy of ADPMC is 5 mm and the unbalanced force F_C is 50 N, the vibration response of M_2 is 96.6 μm at the 3rd order natural frequency and the vibration response of M_2 is 10.4 μm at the 5th order natural frequency.

The vibration responses of points M_1 and M_2 at the 3rd order and 5th order natural frequencies under various operating conditions are analyzed in the previous text. However, regardless of the above-mentioned operating conditions, the vibration responses of points M_1 and M_2 are very small near the operating frequency of 47.5 Hz. For instance, when the radial misalignment Δy of ADPMC is 5 mm and the unbalanced force F_C is 50N, the vibration response of point M_1 is 0.11 μm. Meanwhile, the vibration response of point M_2 is 0.65 μm. It can be seen that the vibration response of the centrifugal pump rotor system fully meets the operating requirements.

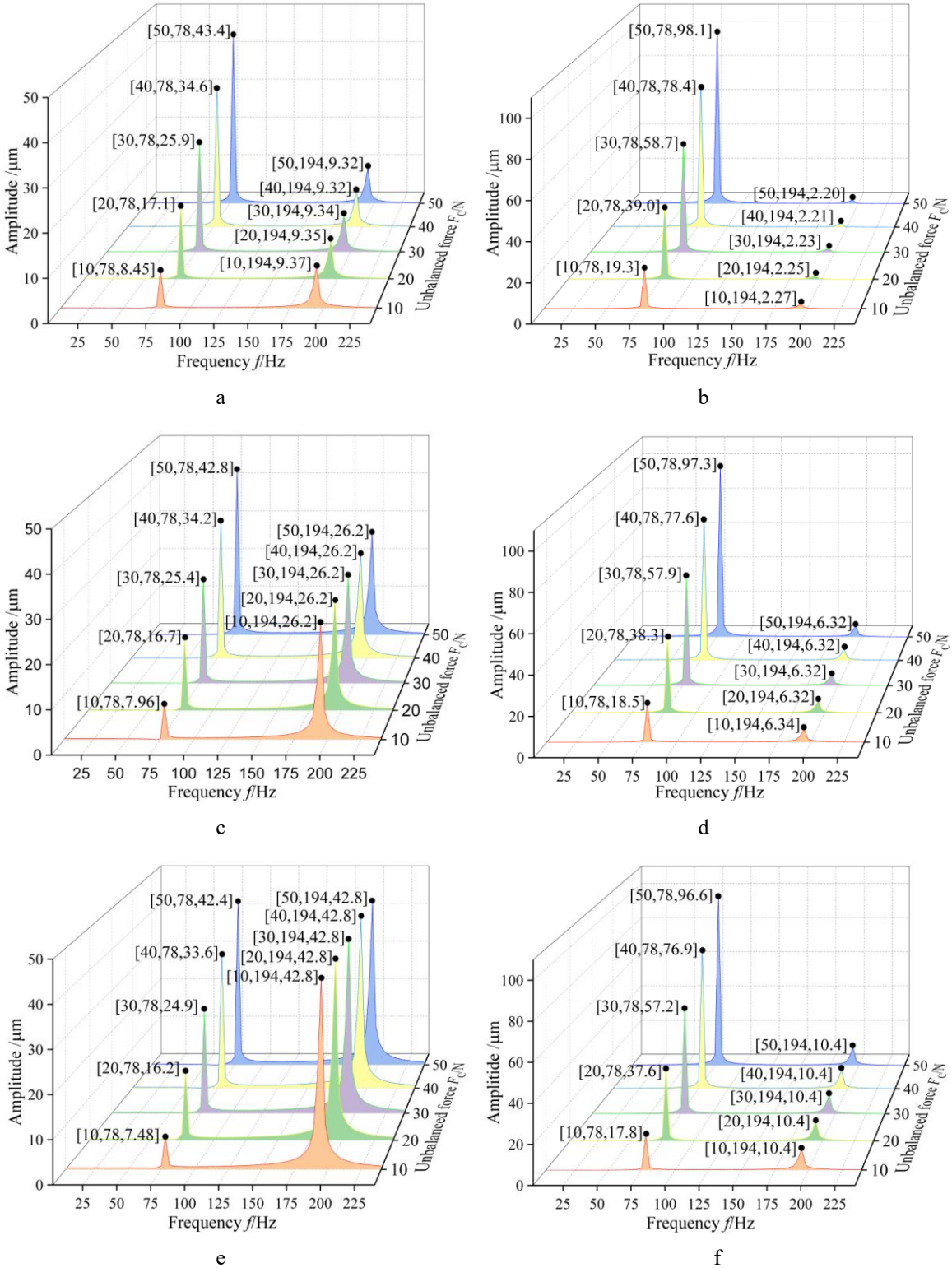

Fig. 14 Vibration spectrum diagrams of monitoring points under dual excitation sources: a – vibration spectrum of point M_1 (Δy = 1 mm), b – vibration spectrum of point M_2 (Δy = 1 mm), c – vibration spectrum of point M_1 (Δy = 3 mm), d – vibration spectrum of point M_2 (Δy = 3 mm), e – vibration spectrum of point M_1 (Δy = 5 mm), f – vibration spectrum of point M_2 (Δy = 5 mm)

7. Conclusions

In this paper, a model of centrifugal pump rotor system driven by ADPMC is developed. The vibration characteristics of centrifugal pump rotor system is studied considering the effects of unbalanced magnetic pull caused by the misalignment of ADPMC and the unbalanced force caused by mass eccentricity of impeller. The main conclusions are as follows:

1. The unbalanced magnetic pull caused by the axial misalignment of ADPMC is large, while the unbalanced magnetic pull caused by the radial misalignment of ADPMC is relatively small. In engineering applications, large radial misalignment is allowed when ADPMC is installed, but large axial misalignment is not allowed.

2. The natural frequencies of the rotor system with the same modal order are basically the same under different operating conditions, which is related to the arrangement of bearings in the rotor system. The first order bending modal shapes of the rotor system is represented by the impeller vibration in the orthogonal direction, and the second order bending modal shapes of the rotor system is represented by the permanent magnet disk vibration in the orthogonal direction.

3. The results of harmonic response analysis show that the vibration displacements of the left and right journal of the centrifugal pump shaft are small under the action of the unbalanced magnetic pull and the unbalanced force of the impeller near the operating frequency, which fully meets the operating requirements. It also shows that ADPMC is not sensitive to the radial misalignment, that is, the large radial misalignment of ADPMC will not result in severe vibration of the rotor system. Therefore, ADPMC has positive isolation vibration characteristics between linked shafts.

Acknowledgements

The work is sponsored by the visiting and training projects for teachers in Jiangsu colleges (Grant No. 2024TDFX009) and the “Blue Project” of Jiangsu Colleges and Universities.

References

1. **Ma, X.; Li, Z.; Xiang, J.; Chen, C.; Huang, F.** 2025. Vibration characteristics of rotor system with coupling misalignment and disc-shaft nonlinear contact, Mechanical Systems and Signal Processing 223: 111839. https://doi.org/10.1016/j.ymssp.2024.111839.
2. **Wang, N.; Jiang, D.; Behdinan, K.** 2017. Vibration response analysis of rubbing faults on a dual-rotor bearing system, Archive of Applied Mechanics 87(11): 1891-1907. https://doi.org/10.1007/s00419-017-1299-9.
3. **Sawalhi, N; Ganeriwala, S; Tóth, M.** 2019. Parallel misalignment modeling and coupling bending stiffness measurement of a rotor-bearing system, Applied Acoustics 144: 124-141. https://doi.org/10.1016/j.apacoust.2017.07.022.
4. **Liu, S.; Ma, Y.; Zhang, D.; Hong, J.** 2012. Studies on dynamic characteristics of the joint in the aero-engine rotor system, Mechanical Systems and Signal Processing 29: 120-136. https://doi.org/10.1016/j.ymssp.2011.12.001.
5. **Lu, H.; Li, W.; Shen, J.; Chen, T.; Sheng, L.** 2023. Dynamic Characteristics Analysis of Rotor-Bearing System Considering Bearing Clearance and Hybrid Eccentricity, Journal of Vibration Engineering and Technologies 12(2): 2249-2263. https://doi.org/10.1007/s42417-023-00977-7.
6. **Xue, X.; Huo, Q.; Liu, J.; Jia, J.** 2021. Nonlinear dynamic load analysis of aviation spline coupling with mass eccentricity and misalignment, Advances in Mechanical Engineering 13(2): 1687814021996511. https://doi.org/10.1177/1687814021996511.
7. **Wang, H.; Gong, J.** 2019. Dynamic analysis of coupling misalignment and unbalance coupled faults, Journal of Low Frequency Noise, Vibration and Active Control 38(2):363-376. https://doi.org/10.1177/1461348418821582.
8. **Desouki, M.; Sassi, S.; Renno, J.; Gowid, S. A.** 2020. Dynamic Response of a Rotating Assembly under the Coupled Effects of Misalignment and Imbalance, Shock and Vibration 2020: 8819676. https://doi.org/10.1155/2020/8819676.
9. **Li, Z.; Li, J.; Li, M.** 2018. Nonlinear dynamics of unsymmetrical rotor-bearing system with fault of parallel misalignment, Advances in Mechanical Engineering 10(5): 1687814018772908. https://doi.org/10.1177/1687814018772908.
10. **Wang, D.; Yang, W.; Yang, J.; Jiang, K.; Zhang, J.; Fu, Y.** 2023. Research on the vibration characteristics and performance optimization of the rotor-shaft system of an unbalanced permanent magnet synchronous motor, Journal of Mechanical Science and Technology 37(9): 4425-4439. https://doi.org/10.1007/s12206-023-0802-1.
11. **Huang, Z.; Zhou, J.; Yang, M.; Zhang, Y.** 2011. Vibration characteristics of a hydraulic generator unit rotor system with parallel misalignment and rub-impact, Archive of Applied Mechanics 81(7): 829-838. https://doi.org/10.1007/s00419-010-0453-4.
12. **Hujare, D. P.; Karnik, M. G.** 2018. Vibration responses of parallel misalignment in Al shaft rotor bearing system with rigid coupling, Materials Today: Proceedings 5(11): 23863-23871. https://doi.org/10.1016/j.matpr.2018.10.178.
13. **Wang, N.; Jiang, D.** 2018. Vibration response characteristics of a dual-rotor with unbalance-misalignment coupling faults: Theoretical analysis and experimental study, Mechanism and Machine Theory 125: 207-219. https://doi.org/10.1016/j.mechmachtheory.2018.03.009.
14. **Wang, Pf.; Yang, Y.; Xu, H.; Ma, H.; Han, Q.; Luo, Z.; Wen, B.** 2023. Effect of static and dynamic misalignment of rolling bearing on nonlinear vibration characteristics of rotor system, Journal of Central South University 30(3):871-903. https://doi.org/10.1007/s11771-023-5268-x.
15. **Xie, Z.; Yang, K.; He, T.; Jiao, J.** 2023. Experimental and theoretical analysis on the nonlinear rotor-dynamic performances and vibration characteristics of a novel bearing-rotor system, Mechanical Systems and Signal Processing 199: 110416. https://doi.org/10.1016/j.ymssp.2023.110416.
16. **Chen, X.; Yuan, S.; Peng, Z.** 2015. Nonlinear vibration for PMSM used in HEV considering mechanical and magnetic coupling effects, Nonlinear Dynamics 80(1-2): 541-552.

https://doi.org/10.1007/s11071-014-1887-y.
17. **Zhang, G.; Kong, K.; Huang, Y.; Liu, H.; Pei, K.** 2017. Dynamic Analysis on the Rotor System of Permanent Magnet Generator in Consideration of Prestress, Bearing (2): 33-36 (in Chinese). https://doi.org/10.19533/j.issn1000-3762.2017.02.009.
18. **Wu, H.; An, Q.** 2008. Calculation on Stiffness of Cylindrical Roller Bearing with EHL, Bearing (1): 1-4 (in Chinese). https://doi.org/10.19533/j.issn1000-3762.2008.01.001.
19. **Luo, Y.; Zhang, W.; Fan, Y.; Han, Y.; Li, W.; Acheaw, E.** 2021. Analysis of Vibration Characteristics of Centrifugal Pump Mechanical Seal under Wear and Damage Degree, Shock and Vibration 2021: 6670741. https://doi.org/10.1155/2021/6670741.

H. Mu, H. Zhai, C. Shen, L. Wu, X. Chu, W. Zhu

VIBRATION CHARACTERISTICS ANALYSIS OF ROTOR SYSTEM WITH PERMANENT MAGNET DRIVE CONSIDERING MISALIGNMENT AND UNBALANCE

S u m m a r y

Misalignment and unbalance are two major mechanical faults in rotating machinery. In recent years, with the increasing application of permanent magnet coupling in rotating machinery, it is necessary to study the misalignment and unbalance of rotor system with permanent magnet drive. In this paper, the vibration characteristics of centrifugal pump rotor system driven by ADPMC considering misalignment and unbalance faults will be discussed. First, the three-dimensional models of ADPMC with axial and radial misalignments are established respectively, and the axial and radial unbalanced magnetic pull of ADPMC are solved. Second, the axial force of angular contact ball bearing and radial force of cylindrical roller bearing are calculated under different operating conditions. Further, the radial support stiffness of each bearing is obtained. Third, the modal analysis of rotor system driven by ADPMC is carried out to obtain the natural frequencies and modal shapes. Finally, the radial unbalanced magnetic pull of ADPMC and unbalanced force caused by mass eccentricity of impeller are taken as the excitation sources, and the harmonic response of rotor system are calculated. The results show that the axial misalignment of ADPMC will cause a larger unbalanced magnetic pull, and the radial misalignment of ADPMC will lead to a smaller unbalanced magnetic pull. When ADPMC has different misalignment faults, the natural frequencies of same modal order of rotor system are basically the same. In the vicinity of the operating frequency, the vibration displacement at two journal of the rotor system excited by dual excitation sources are both small. Therefore, large radial misalignment of ADPMC can be allowed in rotor system, and ADPMC has good vibration isolation characteristics between the driver shaft and the driven shaft. The results provide important engineering references for the application of ADPMC in rotating machinery.

Keywords: ADPMC, misalignment, rotor system, modal analysis, harmonic response, unbalance.

Received March 25, 2025
Accepted August 22, 2025